Multifunctional Nanoparticles for Combining Ultrasonic Tumor Imaging and Targeted Chemotherapy

Natalya Rapoport, Zhonggao Gao, Anne Kennedy

Background Drug delivery in polymeric micelles combined with tumor irradiation by ultrasound results in effective drug targeting, but this technique requires prior tumor imaging. A technology that combined ultrasound imaging with ultrasound-mediated nanoparticle-based targeted chemotherapy could therefore have important applications in cancer treatment.

Methods Mixtures of drug-loaded polymeric micelles and perfluoropentane (PFP) nano/microbubbles stabilized by the same biodegradable block copolymer were prepared. Size distribution of nanoparticles was measured by dynamic light scattering. Cavitation activity (oscillation, growth, and collapse of microbubbles) under ultrasound was assessed based on the changes in micelle/microbubble volume ratios. The effect of the nano/microbubbles on the ultrasound-mediated cellular uptake of doxorubicin (Dox) in MDA MB231 breast tumors in vitro and in vivo (in mice bearing xenograft tumors) was determined by flow cytometry. Statistical tests were two-sided.

Results Phase state and nanoparticle sizes were sensitive to the copolymer/perfluorocarbon volume ratio. At physiologic temperatures, nanodroplets converted into nano/microbubbles. Doxorubicin was localized in the microbubble walls formed by the block copolymer. Upon intravenous injection into mice, Dox-loaded micelles and nanobubbles extravasated selectively into the tumor interstitium, where the nanobubbles coalesced to produce microbubbles with a strong, durable ultrasound contrast. Doxorubicin was strongly retained in the microbubbles but released in response to therapeutic ultrasound. Microbubbles cavitated under the action of tumor-directed ultrasound, which enhanced intracellular Dox uptake by tumor cells in vitro to a statistically significant extent relative to that observed with unsonicated microbubbles (drug uptake ratio = 4.60; 95% confidence interval [CI] = 1.70 to 12.47; $P = .017$) and unsonicated micelles (drug uptake ratio = 7.97; 95% CI = 3.72 to 17.08; $P = .0032$) and resulted in tumor regression in the mouse model.

Conclusions Multifunctional nanoparticles that are tumor-targeted drug carriers, long-lasting ultrasound contrast agents, and enhancers of ultrasound-mediated drug delivery have been developed and deserve further exploration as cancer therapeutics.

J Natl Cancer Inst 2007;99:1095–106

Current tumor chemotherapy is associated with severe side effects caused by drug effects on healthy tissues. In addition, due to anomalous tumor vascularization and high interstitial pressure, spatial drug gradients are created in the tumor volume, resulting in survival of some cancer cells. These cells have a tendency to become drug resistant, thus dramatically decreasing the effect of subsequent treatment rounds. Drug encapsulation has the potential to overcome both obstacles because it not only decreases systemic concentration of free drug but also favors drug accumulation in the tumor volume via the enhanced permeability and retention effect described by Maeda et al. (1) and may modulate intracellular drug trafficking (2,3).

In our previous work, we used polymeric micelles for drug encapsulation (3–12). Polymeric micelles are nanoparticles formed by self-assembly of amphiphilic block copolymers; they have a size between 10 and 100 nm and core–shell structure; and they are most commonly spherical in shape (13). We demonstrated that ultrasonic irradiation of the tumor triggered drug release from micelles and transiently altered cell membrane permeability, resulting in effective intracellular drug uptake by the tumor cells. Furthermore, ultrasound treatment enhanced drug infiltration and diffusion throughout the tumor volume, thus reducing drug concentration gradients (11,12). Successful treatment of drug-sensitive

Affiliations of authors: Department of Bioengineering, University of Utah, Salt Lake City, UT (NR, ZG); Department of Radiology, School of Medicine, University of Utah, Salt Lake City, UT (AK).

Correspondence to: Natalya Rapoport, PhD, DSc, Department of Bioengineering, University of Utah, 20 S. 2030 E. Rm 108, Salt Lake City, UT 84112 (e-mail: natasha.rapoport@m.cc.utah.edu).

See "Funding" and "Notes" following "References."

DOI: 10.1093/jnci/djm043

CONTEXT AND CAVEATS

Prior knowledge

Ultrasound irradiation of drug-encapsulated micelles has shown promise as a means of achieving targeted treatment of tumors in animal models. However, the possibilities of using drug and carrier fomulations that produce (in vivo) both micelles and echogenic microbubbles to encapsulate drug, thus improving drug release and uptake and at the same time providing the imaging modality needed for focused ultrasound treatment of tumors, had not been explored.

Study design

Formulations for producing drug-encapsulated micelles and microbubbles and their response to ultrasound were characterized physically. Then, in vivo experiments were conducted in animal models to measure the extent to which they improved ultrasound-mediated drug uptake in tumors (relative to micellar formulations) and permitted tumor imaging.

Contribution

A novel approach for treatment of tumors that makes use of the echogenic properties of drug carriers to both improve drug uptake and simplify imaging is described.

Implications

The possibilities for targeted drug delivery to tumors based on focused ultrasound of drug-containing echogenic microbubbles deserves further exploration.

Limitations

Additional development and characterization of this experimental approach is required before its possible therapeutic advantages can be determined.

ovarian carcinoma and multidrug-resistant breast cancer in nude mice was achieved using this treatment modality (11,14).

Ultrasound has a number of attractive features as a drug delivery modality. Tumor sonication with millimeter precision is feasible, and ultrasound may be directed toward deeply located body sites in precise energy deposition patterns. Sonication may be performed noninvasively or minimally invasively through intraluminal, laparoscopic, or percutaneous means. For extracorporeal sonication, the transducer is placed in contact with a water-based gel or water layer on the skin, and no insertion or surgery is required.

Ultrasound-mediated chemotherapy as well as all other energy-based tumor treatment modalities requires tumor imaging before treatment. Although this imaging can be performed in a variety of ways, the possibility for combining diagnostic and therapeutic ultrasound for tumor imaging and treatment is especially attractive for reasons of simplicity and cost-effectiveness. Some dual-modality imaging/therapy high-intensity–focused ultrasound (HIFU) instruments have recently been marketed. They are used predominantly for the ablative treatment of prostate, kidney, or uterine tumors. However, ablative techniques present a number of problems related to precise control of heat deposition, and patient motion and breathing during the treatment are problematic.

Here, we describe a therapeutic technique that utilizes ultrasound for targeted drug delivery and tumor imaging. It relies on the instruments that are currently used for HIFU treatment (but at substantially lower ultrasound energies) and novel multifunctional

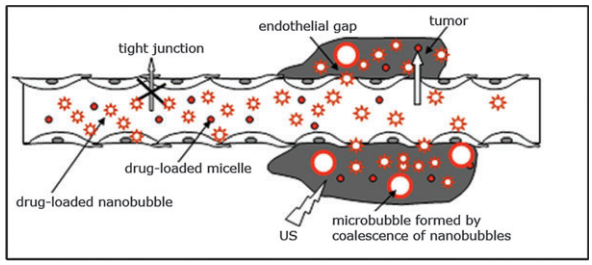

Fig. 1. Schematic representation of drug targeting through the defective tumor microvasculature using the echogenic drug delivery system. The system comprises polymeric micelles (**small circles**), nanobubbles (**stars**), and microbubbles (**large circles**). Micelles are formed by a biodegradable block copolymer (e.g., poly[ethylene glycol]-*block*-poly[L-lactide] or poly[ethylene glycol]-*block*-poly[caprolactone]); bubbles are formed by perfluorocarbon (e.g., perfluoropentane) stabilized by the same (or different) biodegradable block copolymer. Lipophilic drug (e.g., doxorubicin) is localized in the micelle cores and in the walls of nano/microbubbles. The tight junctions between cells in endothelial lining of the blood vessels in normal tissues do not allow extravasation of drug-loaded micelles or nano/microbubbles (indicated by **cross**). In contrast, tumors are characterized by defective vasculature with large gaps between the endothelial cells, which allows extravasation of drug-loaded micelles and small nanobubbles resulting in their accumulation in the tumor interstitium. On accumulation in the tumor tissue, small nanobubbles coalesce into larger, highly echogenic microbubbles.

nanoparticles composed of nanoscale polymeric micelles that function as drug carriers and nano- or microscale echogenic microbubbles that serve as drug carriers, drug delivery enhancers, and ultrasound contrast agents. Drug carrying, tumor targeting, and retention in the tumor volume are functions of the micelles and/or nanobubbles; ultrasound contrast properties are provided by the microbubbles formed in tumor volume by coalescence of nanobubbles. Their structure and properties are discussed below.

These components and their predicted in vivo distribution are schematically illustrated in Fig. 1. The endothelial cells of the blood vessels in normal tissue are joined by tight junctions that prevent penetration of drug-loaded micelles or nano/microbubbles. In contrast, tumors are characterized by a defective vasculature with large gaps between the endothelial cells that allow the extravasation of nanoparticles up to 750 nm in size (15,16). This permeability allows for accumulation of drug-loaded micelles and nanobubbles in the tumor interstitium via the enhanced permeability and retention effect (4,5). As will be shown below, the extravasated nanobubbles coalesce in the tumor volume to form microbubbles that produce strong echo in ultrasound imaging. When subjected to tumor-directed therapeutic ultrasound, the microbubbles oscillate, grow, and collapse in a process called inertial cavitation (17). Inertial cavitation of microbubbles causes a release of microbubble-encapsulated drug, enhances drug release from polymeric micelles (18–23), and perturbs cell membranes (24). Because free drug is internalized much more effectively than encapsulated drug, tumor-localized drug release from microbubbles and micelles results in effective intracellular drug uptake (4,5,7,21–23,25–27).

Using the system described above, a drug could be delivered specifically to the sites irradiated by ultrasound. Because the acoustic energy can be localized to millimeter and even submillimeter volumes in the megahertz frequency range, precise spatial control of drug delivery can be achieved.

The constituents of the system are introduced as a mixture of drug-loaded micelles formed by a biodegradable block copolymer (poly[ethylene glycol]-*block*-poly[L-lactide] [PEG-PLLA], PEG-*block*-poly[caprolactone] [PCL], or others) and nanodroplets that are formed by perfluoropentane (PFP) and stabilized by an outer layer of the same (or a different) block copolymer. Because PFP has a boiling point of 29 °C, upon heating to physiologic temperatures, the PFP nanodroplets vaporize inside the copolymer walls, resulting in conversion of the nanodroplets into nano and/or microbubbles. A loaded drug partitions between micelles and nano/microbubbles.

In vivo, the PFP released upon microbubble collapse would be expected to be eliminated through the lungs, similar to what is observed when perfluoropropane was used in vivo in Optison microbubbles (see http://amershamhealth-us.com). Furthermore, because perfluorocarbons have low partition coefficients in blood, PFP binding to blood proteins would be expected to be minimal. Copolymer micelles gradually disassemble into individual molecules (unimers) due to dilution by body fluids (for example, by lymphatic drainage of the tumor), and the small size of the copolymer molecules (<40 kDa) allows for them to be excreted by the kidneys. Furthermore, the copolymer molecules are biodegradable, and the products of hydrolysis can be excreted through the liver and the kidney.

In the designed formulations, nanodroplet and microbubble sizes and volume fractions are controlled by varying the PFP/copolymer concentration ratio; it was generally observed that at a fixed PFP concentration, droplet size decreased with higher copolymer concentration, and for a fixed copolymer concentration, droplet size increased with higher PFP concentration. In phase diagrams of PFP/copolymer formulations at room temperature, three zones are observed as the PFP/copolymer concentration ratio increased: zone 1 is characterized by micelles with PFP dissolved in the micelle cores and the absence of droplets. In zone 2, micelles and nano/microdroplets coexist. Zone 3 is characterized by the existence of nanodroplets only with a bimodal (lower PFP concentration) or monomodal distribution of bubble sizes.

For therapeutic applications, preparations that fall within the micelle/nanobubble coexistence range (zone 2) and the bimodal part of zone 3 appear to be the most useful because drug-loaded micelles and small nanobubbles are expected to extravasate through the defective tumor microvasculature and accumulate in tumor interstitium. If nanobubbles coalesce in the tumor into micron-size nanoparticles, this could result in a strong ultrasound contrast in tumor ultrasonography. The application of therapeutic ultrasound to tumor after ultrasound imaging is expected to trigger drug release from micelles and microbubbles, ensuring localized drug internalization by tumor cells. Thus, injection of drug-loaded formulations has the potential to allow clinicians to combine ultrasound tumor imaging with ultrasound-mediated targeted chemotherapy.

Materials and Methods

Micelle and Nanoemulsion Preparation

Biodegradable diblock copolymers (PEG-PLLA) and (PEG-PCL) in both of which the molecular mass of the blocks was 2000 d were bought from JCS Biopolytech Inc, Toronto, ON, Canada.

Micelles (empty or Dox-loaded) were formed by a solvent exchange technique. Copolymer (PEG-PLLA or PEG-PCL) without or with doxorubicin (Dox) was dissolved in dimethylsulfoxide or tetrahydrofurane, and the solution was dialyzed against phosphate-buffered saline (PBS) using a membrane with a molecular mass cut-off of 3000 d (Spectra/Por, Spectrum Laboratories Inc, Savannah, GA) to form empty or Dox-loaded micelles. Copolymer concentrations in the micelle preparations ranged from 0.1% to 1.0%. In drug uptake and biodistribution experiments, the copolymer concentration was 5 mg/mL and the Dox concentration was 0.75 mg/mL. For fluorescence microscopy, a Dox concentration of 50 mg/mL was used. The final Dox concentration in micelles was measured by high-performance liquid chromatography using a Supelco LC-18 column (250 × 4.6 mm internal diameter, 5-mm particle size) and a Hitachi high-performance liquid chromatography instrument (D-6000 interface; L-4200H UV-VIS detector; F-1080 Fluorescence Detector; L-6200A intelligent pump, and AS-2000 Autosampler). The mobile phase was a 0.1% acetonitrile–0.1% NaH_2PO_4 solution (40:60 vol/vol) adjusted to pH 3.0 with phosphoric acid, and the flow rate was 1.0 mL/minute. Doxorubicin eluted at 6.2 minutes and was detected by a fluorescence detector with an excitation wavelength of 480 nm and an emission wavelength of 550 nm. Depending on the concentration and type of the copolymer, the sizes of the drug-loaded micelles ranged from 20 to 100 nm in diameter. Drug-loaded micelles were sterilized by filtration through 200-nm filters.

The preparation of drug-loaded nanoemulsion proceeded in three steps. In the first step, drug loading into micelles was performed and the micellar solutions were sterilized by filtration through 200-nm filters. In the second step, liquid perfluorocarbon was sterilized by filtration and an aliquot of sterilized perfluorocarbon was added to the sterilized solution of drug-loaded micelles. Finally, the mixture was sonicated by externally applied 20-kHz ultrasound to produce a nano- or microemulsion. Initially, sonication was performed at room temperature; in subsequent experiments, the samples were sonicated in ice-cold water to reduce foam formation. Preliminary data showed that extending sonication time beyond 60 seconds did not change the properties of the micelle/nanoemulsion systems. The nanoemulsion droplets are heavier than water and precipitate to the bottom of the test tube. Therefore, before taking an aliquot, the nanoemulsion was extensively mixed by pipetting it in and out.

Measurement of Nanoparticle Size Distribution

Particle size distribution was determined based on dynamic light scattering at a scattering angle of 90° using a Malvern Zetasizer 3000 HSA instrument equipped with a 633-nm helium/neon laser and a temperature controller (Malvern Instruments, Inc, Southboro, MA). Measurements were performed at room temperature and at a physiologic temperature range for various combinations of copolymer and PFP. The instrument allows for measurement of particle size distribution in the range of 20 nm–6 μm; microparticles larger than 6 μm might escape registration. However, visual monitoring of the samples at room temperature using an inverted microscope and hemocytometer (model 3200, Hauser Scientific, Horsham, PA) indicated the absence of microdroplets larger than 6 μm. A hemocytometer was also used for measuring mean microdroplet concentration.

To monitor the effect of heating to physiologic temperatures on the particle size distribution, the samples were heated inside the Malvern Zetasizer 3000 HSA instrument to temperatures as high as 42 °C and maintained at the desired temperature for 5 minutes during sizing. Upon completion of the measurement, the samples were cooled back to room temperature and the size measurements were repeated.

Optical and Fluorescence Imaging

For visual monitoring of nanodroplet and microbubble behavior, the formulations consisting of 0.5% PEG-PLLA/2% PFP were placed in closed plastic capillary tubes (internal diameter of 340 μm) of snake mixer slides (XXS, Zweibrucken, Germany) and examined under the ×100 magnification using a Nikon Fluophot fluorescence microscope (Nikon USA, Melville, NY) equipped with a sample heating stage TCS-100 (AmScope, Chino, CA) that provided for sample heating up to 50 °C. In the experiments involving the cells, a droplet of a cell suspension was first premixed with a desired Dox-containing PBS solution or microbubble formulation and then placed in the capillary tube of the mixer slide. In the experiments involving sonication, unfocused ultrasound was applied through the Aquasonic coupling gel (Parker Laboratories, Inc, Orange, NJ) to the region of the slide outside of the visual field; note that in these experiments, sonication proceeded in a near field, and therefore, the ultrasound energy experienced by the sample could be different from the nominal output energy indicated by the ultrasound-generating instrument.

Sonication

Two types of ultrasound transducers were used. Unfocused 1- or 3-MHz ultrasound was generated by an Omnisound 3000 instrument (Accelerated Care Plus Inc, Sparks, NV) equipped with a 1-cm^2 piezoceramic crystal and 5-cm^2 transducer head. Focused 1.1- or 3.3-MHz ultrasound was generated by a submersible focused piezoceramic transducer (model H-101 S/N-29, Sonic Concepts, Woodinville, WA).

Monitoring of Cavitation Activity

The microbubble formulation was drawn into a Samco polyethylene transfer pipette (5 mm internal diameter, 0.3 mm wall thickness, and 1.5 cm height, Fisher Scientific, Pittsburg, PA). Using a three-way micropositioner (Velmex, Bloomfield, NY), the transfer pipette was positioned in the focal zone of the focusing transducer. The transducer was housed in an open glass tank (31 × 28 × 51 cm) containing approximately 20 L of filtered distilled water maintained at room temperature (23–24 °C) or 37 °C. To minimize possible standing wave formation, a 2.5-cm thick rubber liner was mounted opposite the transducer. Electronic sinusoidal waveform of 1.1- or 3.3-MHz frequency was generated by a programmable generator (model F33, Interstate Electronics Corporation, Anaheim, CA) and triggered by a function generator (model 3314A, Hewlett Packard, Loveland, CO). The signal was amplified by a power amplifier (model 240L, Electronic Navigation Industries, Rochester, NY). Ultrasound pressure was controlled by varying the amplitude of the drive signal to the transducer.

For measurement of the ultrasound energy exposure, root-mean-square negative pressure was measured at the focal site of the transducer using a piezoceramic needle hydrophone with a geometrical diameter of 1.5 mm (model TNU100A, NTR Systems, Seattle, WA). With focused ultrasound, the sonication volume was more than an order of magnitude smaller than the total volume of the sample (400 mL); however, ultrasound-induced microstreaming caused sample stirring, which reduced nonuniformity of the sonication throughout the sample volume.

For measurement of cavitation intensity under unfocused ultrasound, the Omnisound 3000 transducer probe was positioned at a distance of 1 cm from the Samco transfer pipette inserted in a water tank at 37 °C. Cavitation intensity was characterized according to the micelle/microbubble volume ratio as described in the "Results."

To determine if the drug that is released upon microbubble collapse remains free in solution or is re-encapsulated by the reformed micelles, the drug-loaded sonicated samples were dialyzed against PBS and the Dox dialysis rates were compared with those of free Dox and micelle-encapsulated Dox.

Cells

Breast cancer MDA MB231 and ovarian cancer A2780 cells were obtained from American Type Culture Collection (Manassas, VA). MDA MB231 cells were cultured in Leibovitz's L-15 medium with 2 mM L-glutamine supplemented with 10% fetal bovine serum (FBS) at 37 °C in air. A2780 cells were cultured in RPMI-1640 medium supplemented with 10% FBS at 37 °C in humidified air containing 5% CO_2.

Animal Procedures

Thirty nu/nu mice 4–6 weeks old were bought from Charles River Laboratories (Wilmington, MA). Animals were housed in accordance with the Guide for the Care and Use of Laboratory Animals as adopted by the National Institutes of Health. All experiments were performed in accordance with the guidelines of the Institutional Animal Care and Use Committee of the University of Utah (Protocol 05-01002). For inoculation, breast cancer MDA MB231 cells or ovarian carcinoma A2780 cells were suspended in 100 mL serum-free RPMI-1640 medium and inoculated subcutaneously to the flanks of unanesthetized mice (2×10^6 cells per mouse).

Three mice bearing breast cancer xenograft tumors were used as controls. Eight mice bearing breast cancer xenograft tumors were used to monitor the effect of ultrasound on tumor growth after the intravenous injections of microbubble-encapsulated Dox when tumor volume reached 100–150 mm^3 (1.5 months after cell inoculation). These mice were treated by four intravenous injections of 3 mg/kg Dox encapsulated in 0.5% PEG-PLLA/2% PFP microbubbles injected twice weekly. Three of the eight mice were not sonicated; in the other five mice, the tumors were sonicated by 3-MHz unfocused ultrasound (power density 2 W/cm^2, duty cycle 20%, ultrasound exposure time 30 seconds); ultrasound was applied 4 hours after the drug injection, and tumor growth/regression rates were monitored.

Three mice bearing breast cancer xenograft tumors were used to measure the effect of ultrasound on the intracellular uptake of Dox in vitro when tumors reached a volume of 1400–1500 mm^3 (2.5–3 months after cell inoculation). Five mice bearing breast cancer xenograft tumors were used to measure the effect of ultrasound

on the Dox uptake by tumor cells and biodistribution in vivo when untreated tumors reached a volume of 500 mm^3 (about 2.5 months after the cell inoculation).

When tumors in seven additional mice that were inoculated with MDA MB231 cells reached a volume of approximately 2000–2500 mm^3 (3 months after the cell inoculation), these mice were used for the contrast-enhanced ultrasound tumor imaging experiments. Subsequently, four additional mice were inoculated with MDA MB231 cells and one was inoculated with A2780 cells to monitor contrast-enhanced ultrasound tumor imaging at earlier stages of tumor growth.

Measurement of Intracellular Drug Uptake by Tumor Pieces In Vitro

The intracellular uptake of Dox was measured when untreated MDA MB231 breast cancer xenograft tumors reached a volume of 1400–1500 mm^3 (between 2.5 and 3 months after the cell inoculation). The mice were killed by cervical dislocation. Immediately after the tumors were excised, tumor pieces of approximately equal size, shape, weight, and orientation in relation to the tumor volume (i.e., directed from the surface toward the center) were prepared using an open glass tube as a tumor cutter. Tumor pieces (20–750 mg in various experiments) were weighed and placed either in Samco polyethylene transfer pipettes or 5-mL plastic test tubes filled with 400 mL (transfer pipettes) or 4 mL (test tubes) of micellar or nanoemulsion Dox formulation. The tumor containers were placed in a water tank maintained at 37 °C. The unfocusing Omnisound 3000 transducer probe was positioned at a distance of 1 cm from the sample. The samples were incubated from 15 to 45 minutes at 37 °C in the corresponding formulation before ultrasound application. "Sham" control exposures were conducted using the same protocol, without ultrasound.

Ten minutes after completion of sonication, tumor pieces were removed from the container, dried on filter paper, digested with 1.0% trypsin to produce individual cells, and fixed in 2.5% glutaraldehyde. Then, cells were filtered through nylon mesh, and cell fluorescence was measured using a FACScan flow cytometer (Becton Dickinson, Franklin Lakes, NJ). In control experiments, we found that intracellular Dox fluorescence is proportional to intracellular Dox uptake (11). The flow cytometry does not provide absolute fluorescence values; the measured value for the same sample may vary from day to day due to the variations in the instrument setting and sensitivity. Therefore, flow cytometry histograms for a particular series of samples were recorded on the same day with the same instrument setting.

The following experiments were performed. 1) Pieces of an excised MDA MB231 tumor (150 mg each) were inserted in 0.4 mL of a medium comprising Dox at a concentration of 0.75 mg/mL encapsulated in PEG-PLLA 0.5% micelles or PEG-PLLA 0.5%/PFP 2% microbubbles. The microbubble concentration was 5×10^8/mL. The samples were preincubated at 37 °C for 15 minutes before 3-MHz unfocused ultrasound was applied for 30 seconds at a nominal output space-average-time-average (SATA) power density of 2 W/cm^2 with a duty cycle of 50%. 2) Large pieces (750 mg each) of an excised MDA MB231 tumor were inserted in 2.5 mL of a medium comprising Dox at a concentration of 0.75 mg/mL encapsulated in PEG-PLLA 0.5% micelles or PEG-PLLA 0.5%/PFP 2% microbubbles. The microbubble concentration was 5×10^8/mL; samples were preincubated at 37 °C for 15 minutes before 3-MHz unfocused ultrasound was applied for a 30-second exposure time at a nominal output SATA power density of 2 W/cm^2 with a duty cycle of 20%.

Measurement of the Intracellular Drug Uptake and Drug Biodistribution In Vivo

Five mice bearing MDA MB231 breast cancer tumors were used in these experiments. Drug distribution experiments were performed when tumors reached a size of about 500 mm^3 (2.5 months after the cell inoculation). Two mice were injected with a micellar Dox formulation (0.75 mg/mL Dox/0.5% PEG-PLLA), and two other mice were injected with the microbubble formulation (0.75 mg/mL Dox/0.5% PEG-PLLA/2% PFP); microbubble dose was about $5x10^7$ bubble/mouse; injected Dox dose was 3 mg/kg. A fifth tumor-bearing mouse was injected with PBS and used as a control. Four hours after the injection, tumors of half of the mice were sonicated by unfocused 3-MHz ultrasound at 2 W/cm^2 power density and 20% duty cycle for a total of 150 seconds to produce ultrasound exposure of 30 seconds; ultrasound was applied to the tumor through the Aquasonic coupling gel. "Sham" exposures were conducted according to the same protocol, but no ultrasound was applied.

Ten minutes after the completion of sonication, tumors and organs (heart, liver, and kidney) of all mice were excised, cut into pieces, and treated to produce individual cells as described above for the in vitro experiments on the intracellular drug uptake. Briefly, tumors and organs were dried on filter paper, digested with 1.0% trypsin to produce individual cells, and fixed in 2.5% glutaraldehyde. Then, cells were filtered through nylon mesh, and cell fluorescence was measured using a FACScan flow cytometer. In earlier experiments on drug biodistribution (4) that were run in duplicate or triplicate, a very low scatter of mean cell fluorescence (<10%) was observed both in vitro and in vivo in samples from different mice that were processed identically. Therefore, in this study, a total of five mice with one mouse per experimental point were used to measure the effect of ultrasound on the intracellular drug uptake and biodistribution in vivo.

Measurement of the Intracellular Drug Uptake by Cells in Suspension or Monolayers

A2780 or MDA MB231 cells suspended in media comprising micelle- or microbubble-encapsulated Dox were drawn into Samco transfer pipettes and positioned in the focal zone of the focusing transducer as described in Monitoring of Cavitation Activity. After sonication, the cells were fixed by 2.5% glutaraldehyde.

The cells grown in monolayers in the wells of 6-well plates to 75% confluence were sonicated at room temperature by unfocused 3-MHz ultrasound applied to the bottom of the well through the Aquasonic coupling gel. After sonication, the cells were processed as described above for tumor pieces. Cell fluorescence was measured by flow cytometry.

Statistical Analysis

The statistical treatment of the intracellular drug uptake data was performed by the Biostatistic Shared Resource, Huntsman Cancer Institute, Salt Lake City, UT. Statistical significance of the

differences in the intracellular drug uptake for micelles versus microbubbles and for nonsonicated versus sonicated samples was analyzed by a two-sided paired *t* test on a logarithmic scale using R2.4.0 software. The effect of microbubbles and ultrasound on the intracellular drug uptake was evaluated for each cell sample by using micellar delivery without ultrasound as a reference. Across the samples, the mean ratios I_{DS}/I_m of the drug uptake observed for a particular delivery system to the drug uptake observed for micelles were calculated.

Statistical treatment of the tumor growth data was performed using Excel 2003 (Microsoft, Redmond, WA), and mean tumor volumes and 95% confidence intervals (CIs) were calculated. *P* values for differences in the tumor growth rates determined by Student's *t* test are presented in the text.

Ultrasound Imaging

Imaging experiments were performed using a 14-MHz linear transducer (Acuson Sequoia 512) and MDA MB231 breast cancer or A2780 ovarian cancer bearing mice in which tumors have been allowed to grow for 3 months to reach the volume of 2000–2500 mm^3; imaging was performed 3, 10, and 12 weeks after the cell inoculation; the microbubble formulations (0.5% PEG-PLLA/2% PFP) were injected intravenously or intratumorally (injection volume 100 or 200 mL, microbubble concentration 10^8–10^9/mL); imaging was performed at various time points after the contrast injections (3 minutes, 18 minutes, 4 hours, 28 hours, 48 hours).

Results

Conversion of Nanodroplets to Microbubbles Upon Heating to Physiologic Temperatures

We studied nanodroplet to microbubble conversion in micelle/nanodroplets formulations using dynamic light scattering and optical microscopy. Dynamic light scattering indicated that sample heating from room temperature to physiologic temperatures did not affect micelle sizes, but resulted in an increase of nanodroplet sizes due to PFP vaporization inside the droplet walls formed by block copolymers. For example, upon heating of a 1% PEG-PLLA/0.5% PFP formulation to 42 °C, nanodroplet/microbubble conversion resulted in an increase of mean particle size from 691 nm (nanodroplets) to 1.24 mm (microbubbles). Upon heating a 1% PEG-PCL/1% PFP formulation to 37 °C, mean particle size increased from 428 nm (nanodroplets) to 1.03 mm (microbubbles). With short-term (5 minutes) heating, nanodroplet/microbubble conversion was reversible—the initial particle size distribution was restored upon cooling (data not shown). However, with longer heating or higher temperatures, microbubble coalescence resulted in the irreversible formation of larger microbubbles (Fig. 2). Micrographs were taken during the heating-cooling-heating cycle of a 0.5% PEG-PLLA/2% PFP sample placed in a closed plastic capillary. At the x100 magnification that was maximal at the current instrument setting, nanodroplets of the initial formulation were not resolved (Fig. 2, A). Visible microbubbles appeared at temperatures above the PFP boiling temperature of 29 °C, and, at this temperature, structural rearrangements were manifested by a vigorous liquid motion inside the capillary. During further heating, large microbubbles grew by attracting and coalescing with small ones (Fig. 2, B and C), which was especially pronounced at hyperthermia conditions (above 42 °C). Upon cooling the sample back from 50 °C to room temperature, the initial structure was not restored; structural rearrangements resulted in a development of a large number of small microdroplets formed via the disintegration of large microbubbles (Fig. 2, D). During the second heating step, large microbubbles grew again by attracting and coalescing with small bubbles, whose number constantly decreased (Fig. 2, E and F). In contrast to the thermodynamically driven reversible PFP evaporation/condensation at 29 °C, the coalescence of the microbubble was an irreversible process, and upon cooling, the system did not return to the original state shown in Fig. 2, A. Irreversible bubble coalescence was also observed at room temperature upon the application of ultrasound (data not shown). A similar effect called acoustic droplet vaporization has recently been described (28–30). For ultrasound imaging purposes, the coalescence of the nano- and microbubbles is a positive factor because the echogenic properties of the nanobubbles increase upon coalescence into the microbubbles. However in therapeutic applications, long-term survival of nanobubbles at physiologic temperatures is required for sufficient accumulation of the nanobubbles in the tumor interstitium.

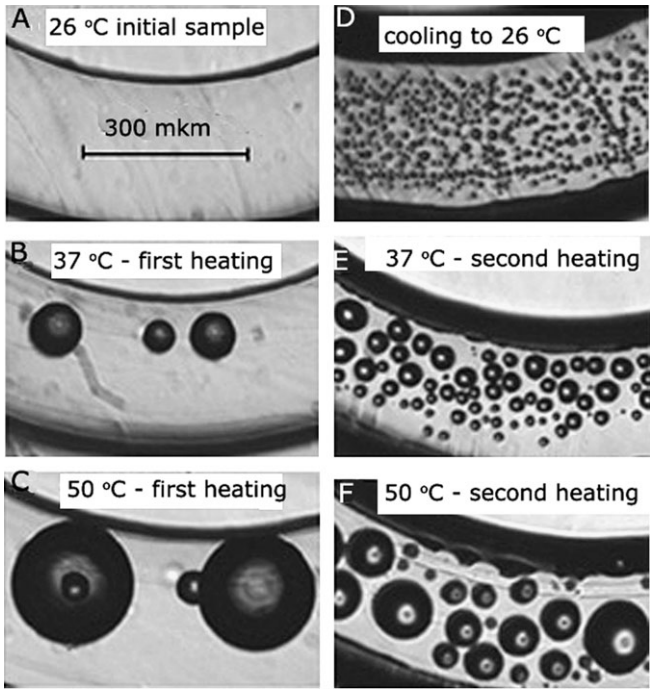

Fig. 2. Optical images of a 0.75 mg/mL Dox/0.5% PEG-PLLA/2% perfluoropentane formulation placed in a closed plastic capillary (internal diameter 340 mm) of a snake mixer slide. The sample was visualized during a heating/cooling/heating cycle using a heating stage and a fluorescence microscope. **A**) At 26 °C, nanodroplets of the initial 0.5%PEG-PLLA/2% PFP formulation were not resolved at the highest available magnification (×100). **B** and **C**) Upon heating to 37 °C (**B**) and 50 °C (**C**), large bubbles grew by attracting and coalescing with small ones. **D**) After the sample was cooled back to room temperature, the initial structure was not restored and a large number of small microdroplets were formed via disintegration of large microbubbles and PFP condensation inside the bubble walls. **E** and **F**) Images were taken during a second heating step at 37 °C and 50 °C, respectively; growth of large microbubbles via the attraction and coalescence with small ones was manifested by a progressive decrease in the number of small microbubbles.

Stability of the Dox-loaded nanobubbles used in in vivo studies (0.75 mg/mL Dox/0.5% PEG-PLLA/2% PFP) was tested by incubating them at 37 °C in closed test tubes for various time periods followed by particle sizing at room temperature. After a 4-hour incubation at 37 °C, the nanobubbles were still present in the formulation and the change in mean nanobubble size was less than 15% (data not shown). Long-term survival of the nano- and microbubbles in vivo was confirmed in ultrasound imaging experiments (see below).

Cavitation Effects

In the context of drug delivery and tumor therapy, inducing localized cavitation in the tumor volume is desirable because it enhances drug release from carriers and perturbs cell membranes, thus considerably increasing intracellular drug uptake. Drug release from micelles starts below the inertial cavitation threshold but is substantially enhanced by inertial cavitation (7,10,18,23,31). We sought to determine ultrasound parameters that induced efficient inertial cavitation. To ascertain the induction of cavitation, we first performed sonication by strong continuous wave focused 1.1-MHz ultrasound at a 4-MPa negative pressure in the focal zone. Sonication was performed at 37 °C (this temperature was above the nanodroplet/microbubble conversion temperature, and therefore microbubbles were present in the system); particle size distribution in the range of 20 nm–6 μm was measured at room temperature before and after sonication (Fig. 3). In the initial 0.2% PEG-PLLA/0.5% PFP formulation, 96.6% of droplets were microdroplets (mean diameter = 1.37 mm). There was a small fraction (3.4%) of nanoparticles (mean diameter = 125 nm). Ultrasound resulted in a decrease of the microdroplet volume fraction from 96.6% to 49% accompanied by the formation of micelles (47.8% of sized particles) with a mean diameter of 46 nm. The volume fraction of 100- to 200-nm nanoparticles (3.2%) remained unchanged (Fig. 3). These data indicate that the copolymer molecules that were released upon collapse of the microbubbles re-assembled into the micelles. These results indicate that ultrasound-induced changes in the micelle/microbubble volume fraction ratio are an indicator of inertial cavitation activity.

In additional experiments, we observed that the inertial cavitation threshold for microbubbles stabilized by PEG-PCL copolymer was higher than that for microbubbles stabilized by PEG-PLLA copolymer (data not shown). Moreover ultrasound frequency, negative pressure, and duration of exposure strongly affected inertial cavitation activity (data not shown).

This method for monitoring cavitation activity was applied to optimize sonication conditions for drug uptake and tumor growth studies. The cavitation activity was compared for 1- and 3-MHz unfocused ultrasound at the same nominal SATA power density of 2 W/cm^2 as specified by the Omnisound 3000 instrument manufacturer. Because the inertial cavitation threshold was higher for microbubbles stabilized by PEG-PCL than for those stabilized by PEG-PLLA copolymer, a PEG-PCL/PFP formulation was chosen to ensure that inertial cavitation conditions would be generated in studies of drug uptake and tumor growth. Ultrasound was applied at 37 °C. The initial composition consisted of micelles with a mean diameter of 36.4 nm (33.9%) and microdroplets with a mean diameter of 1.1 μm (59.3%), and there was also a small fraction (6.8%) of nanodroplets with mean diameter of 198 nm. After sonication for 30 seconds with 1-MHz continuous-wave ultrasound, microbubble collapse resulted in a decrease of the microdroplet volume fraction to 35.4% while that of the micelles increased to 64.6%. With 3-MHz sonication, the microdroplet volume fraction dropped to 13.6%, and that of the micelles increased to 83.2%. Therefore, because of the stronger cavitation activity at 3 MHz, this frequency was chosen for both in vitro and in vivo studies of the effect of ultrasound on intracellular drug uptake and drug biodistribution.

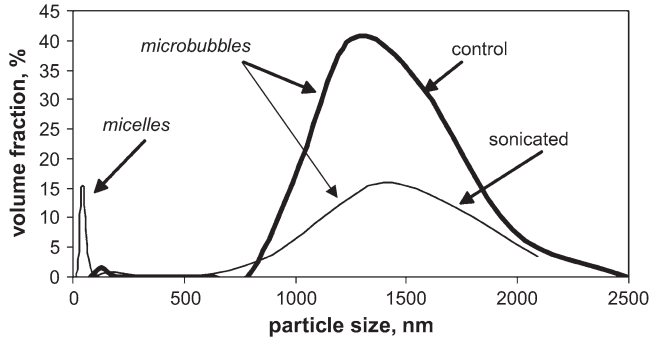

Fig. 3. Effect of 1.1-MHz continuous wave focused ultrasound on the microbubble collapse in 0.2% PEG-PLLA/0.5% perfluoropentane formulation. Ultrasound of 4-MPa space-average-time-average negative pressure was applied for 30 seconds at 37 °C. Particle distribution measurements were performed before and after sonication at room temperature. The initial formulation comprised predominantly microdroplets of 1.37-mm mean diameter (96.6%) and a small fraction of nanodroplets of 125-nm mean diameter (3.4%). Ultrasound-induced microbubble collapse resulted in a decrease of the microdroplet volume fraction from 96.6% to 49% and was accompanied by a formation of micelles with a mean diameter of 46 nm (47.8%). The volume fraction of the 100- to 200-nm nanoparticles (3.2%) remained essentially unchanged.

Drug Distribution and Release

In a micelle formed by block copolymer, Dox is localized in the central hydrophobic compartment (micelle core) (6,9,27). Using fluorescence microscopy, we determined the localization of Dox in the microbubbles. We studied Dox localization in the same formulation (0.75 mg/mL Dox/0.5% PEG-PLLA/2% PFP) that was used in our studies of drug uptake and tumor growth. At room temperature, the nanoparticles in the formulation were not resolved by fluorescence microscopy. When the formulation was heated to 44 °C, coalescence of the nanobubbles resulted in the formation of visible microbubbles (Fig. 4, A) and Dox fluorescence was localized in the microbubble walls formed by the bubble-stabilizing block copolymer. When the microbubbles collapsed under the action of ultrasound, copolymer molecules were released and they re-assembled into the micelles as indicated by dynamic light scattering. Drug was also released from the collapsed microbubbles, and in the absence of cells, the restored micelles re-encapsulated released drug as indicated by a slow rate of Dox dialysis from the sonicated samples (data not shown).

We sought to determine whether the released drug would be internalized by cells that were present during the collapse of the microbubbles. We monitored fluorescence of breast cancer

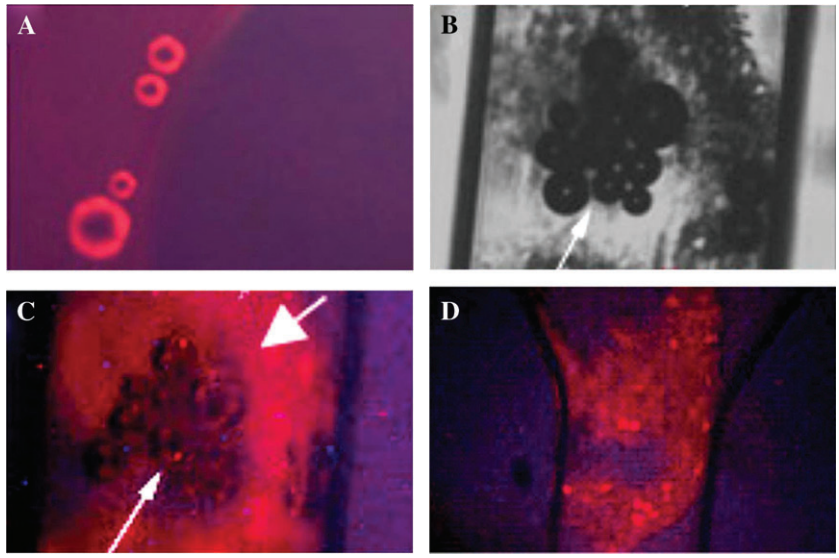

Fig. 4. Fluorescence images of the 0.75 mg/mL Dox/0.5% PEG-PLLA/2% perfluoropentane formulation placed in a plastic capillary (internal diameter 340 mm) of a snake mixer slide. The initial formulation was characterized by a bimodal distribution of nanoparticle sizes (250 and 750–800 nm), and the nanoparticles were not visible at the ×100 magnification that was maximal for the experimental setting. **A**) Heating the formulation to 44 °C resulted in a formation of large (tens of microns) microbubbles due to coalescence of the nanobubbles. The doxorubicin-derived fluorescence (**red**) of the microbubbles was clearly localized in the bubble walls formed by the bubble-stabilizing copolymer. **B**) Optical image of the MDA MB231 cell and bubble aggregates (**arrow**) formed in the capillary during a 150-second sonication (corresponding to a 30-second ultrasound exposure time) by 3-MHz ultrasound at a 2 W/cm^2 nominal space-average-time-average power density with a 20% duty cycle. Ultrasound was applied directly to the slide through the Aquasonic coupling gel. The actual power density experienced by the sample may be different from nominal because the sonication proceeded in the ultrasound near field. **C**) Fluorescence image of the same sample site as presented in B with focus on the bubbles (**thin arrow**). Fluorescence of the bubbles decreased whereas the cells (**thick arrow**) acquired strong fluorescence after sonication. **D**) Fluorescence image of another cell aggregate with the focus on the cells. When the sample was exposed to ultrasound, doxorubicin was internalized by the cells as indicated by the red fluorescence.

MDA MB231 cells inserted into a suspension of Dox-loaded microbubbles placed in a plastic capillary at 37 °C and either treated (Fig. 4, B–D) or not treated with ultrasound. Without ultrasound, the cells did not acquire any fluorescence during a 30-minute observation. However, a strong cellular fluorescence (Fig. 4, C and D) was observed after a 30-second sonication of the capillary plate by 3-MHz ultrasound at a nominal output SATA power density of 2 W/cm^2. These experiments suggested that in the absence of ultrasound Dox was strongly retained by the microbubbles and that the Dox that was released under the action of ultrasound was internalized by the cells.

Microbubbles as Enhancers of Ultrasonic Drug Delivery

Next, we compared ultrasound-mediated intracellular drug uptake by tumor cells when Dox was delivered in microbubbles with uptake when Dox was delivered in micelles. The doxorubicin uptake was characterized by the intracellular fluorescence calculated as the difference between the measured fluorescence of experimental tumor cells and the autofluorescence of corresponding control tumor cells. The experiments were performed for five different cancer samples (excised breast cancer tumors, in vivo breast cancer tumors, breast cancer and ovarian carcinoma cells in monolayers or suspensions as described in Methods). Histograms and data on cell fluorescence for nonsonicated and sonicated samples are presented in Supplementary Figs. 1–3 and in Supplementary Table 1 (available online). For sonicated pieces of an excised MDA MB231 tumor (tumor piece weight, approximately 125 mg), microbubble/ultrasound delivery resulted a greater than twofold enhancement of the intracellular doxorubicin uptake compared with micelle/ultrasound delivery (89 versus 38 arbitrary units) and about a fivefold increase over delivery in micelles without ultrasound (89 versus 19 arbitrary units). Histograms of cell fluorescence for nonsonicated and sonicated cells are presented in Supplementary Fig. 2 (available online).

For large breast cancer tumor pieces (weight ~750 mg), only microbubble/ultrasound delivery resulted in a measurable increase in cell fluorescence over the autofluorescence of control cells.

Ultrasound-induced enhancement of the intracellular doxorubicin uptake by the tumor cells was also observed in vivo. Doxorubicin was injected intravenously into four MDA MB231 tumor-bearing mice; a fifth tumor-bearing mouse was used as a control. Two mice were injected with a micellar doxorubicin formulation (0.75 mg/mL Dox/0.5% PEG-PLLA), and the two other mice were injected with the microbubble formulation (0.75 mg/mL Dox/0.5%/PEG-PLLA/2% PFP; at room temperature this formulation comprised nanodroplets of two sizes, 250 and 750 nm, as determined by light scattering). Four hours after the drug injection, the tumor of one mouse in each treatment group was sonicated by 3-MHz ultrasound at a nominal output SATA power density of 2 W/cm^2 and duty cycle of 20% for a 30-second ultrasound exposure; the other mouse was not sonicated. After removal of the tumor, kidney liver, and heart, the individual cells were produced by tissue digestion with trypsin; the cells were fixed with glutaraldehyde and cell fluorescence was measured by flow cytometry as described in detail in Methods. The results showed that 1) without ultrasound, for both the micellar and microbubble formulation, the fluorescence of the experimental tumor cells was close to the autofluorescence of the control cells signifying low intracellular drug uptake; 2) the application of ultrasound enhanced the intracellular drug uptake by the tumor cells in the presence of both the micellar and microbubble formulation; and 3) the intracellular drug uptake by sonicated samples was substantially higher for the microbubbles compared with micelles (13 versus 7 arbitrary units). No measurable doxorubicin fluorescence was observed in the cells of kidney, liver, or heart, indicating a substantial degree of drug targeting to tumors. The strong effect of the microbubbles indicated that they were preserved in vivo for at least 4 hours, and this was further confirmed by ultrasound imaging experiments described below. Histograms of

Table 1. Statistical analysis of the intracellular drug uptake data (N = 4)

Comparison	Mean ratio	95% CI	*P* value
M	1.00	referent	n/a
Mb vs M	1.73	0.59 to 5.09	.231
M/US vs M*	2.64	0.91 to 7.66	.063
Mb/US vs Mb	4.60	1.70 to 12.47	.017
Mb/US vs M/US	3.02	1.46 to 6.26	.017
Mb/US vs M	7.97	3.72 to 17.08	.0032
(M + Mb)/US vs (M + Mb)	3.48	1.71 to 7.08	.0026

* Statistical analysis was performed on logarithmic scale using R2.4.0 software. The average values calculated this way are geometric means on the original scale. CI = confidence interval; M = micelles; Mb = microbubbles; n/a = not applicable; US = ultrasound.

cell fluorescence for nonsonicated and sonicated cells are presented in Supplementary Fig. 3 (available online).

Even without ultrasound, the intracellular doxorubicin uptake from the microbubbles was often slightly higher that that from the micelles (Supplementary Table 1, available online), presumably due to the presence of some free drug that was released from micelles during nanoemulsion preparation.

The statistical significance of the differences associated with individual treatments across the collection of samples were analyzed by a two-sided paired *t* test on a logarithmic scale using R2.4.0 software (Table 1). Without ultrasound, no differences were observed between drug delivery outcomes for the micelles and microbubbles ($P = .231$). By contrast, for the sonicated samples, the intracellular drug uptake observed for the microbubbles was statistically significantly higher than that observed for the micelles (ratio of uptake = 3.02; 95% CI = 1.46 to 6.26; $P = .017$). The effect of ultrasound on the intracellular drug uptake from micelles, though always positive, was not statistically significant ($P = .063$); however, ultrasound caused a statistically significant increase in the intracellular drug uptake from microbubbles (ratio of drug uptake from microbubbles in the presence of ultrasound versus drug uptake from microbubbles in the absence of ultrasound = 4.60; 95% CI = 1.70 to 12.47; $P = .017$). Statistically significant enhancement of the intracellular drug uptake was also observed when doxorubicin uptake in the presence of microbubbles and ultrasound was compared with that observed with micelles in the absence of ultrasound (ratio of drug uptake = 7.97; 95% CI = 3.72 to 17.08; $P = .0032$). Finally, when the micelle and microbubble delivery systems were analyzed together, the effect of ultrasound on the intracellular drug uptake was statistically significant (ratio of drug uptake = 3.48; 95% CI = 1.71 to 7.08; $P = .0026$).

Combination Chemotherapy by Drug-Loaded Microbubbles and Ultrasound

We next sought to determine if combining microbubble drug delivery with ultrasound would exert effects on tumor growth in vivo. In these experiments, 11 mice bearing MDA MB231 breast tumors were randomly assigned to three groups when tumor volume reached about 100–150 mm^3 (1.5 months after cell inoculation). The control group (n = 3) was intravenously injected with PBS. The other group (n = 8) was given four intravenous twice

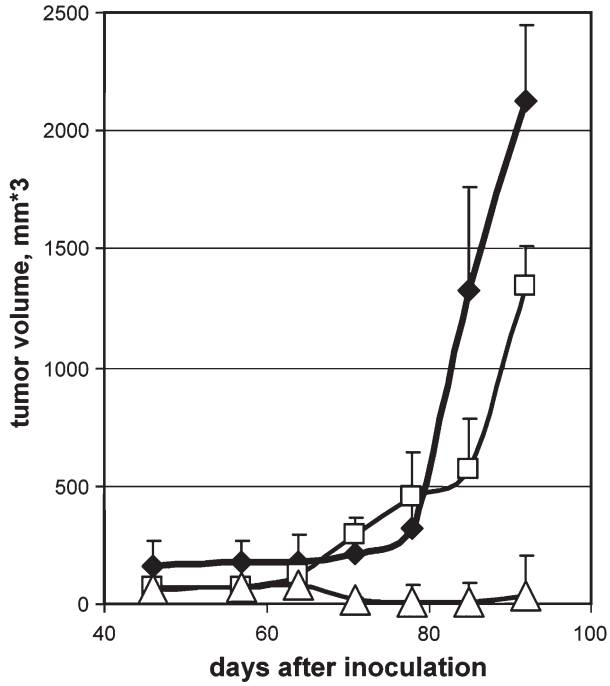

Fig. 5. The effect of ultrasound on tumor growth in mice treated with microbubble-encapsulated doxorubicin. Tumor growth curves for control mice (**filled diamonds**, n = 3); mice treated by four tail vein injections of 100 mL Dox-loaded microbubbles (0.75 mg/mL Dox/0.5% PEG-PLLA/2% perfluoropentane) administered twice weekly without ultrasound (**open squares**, n = 3); and mice treated by the same regimen combined with tumor sonication by 3-MHz ultrasound for a 30-second ultrasound exposure time at a 2 W/cm^2 nominal space-average-time-average power density and 20% duty cycle (**open triangles**, n = 5) were plotted; mean values ± 95% confidence intervals are shown.

weekly injections of microbubble-encapsulated doxorubicin (3 mg/kg) using a formulation consisting of 0.75 mg/mL Dox/0.5% PEG-PLLA/2% PFP. Three of these mice were not treated by ultrasound; the remaining five were treated for 30 seconds with 3-MHz ultrasound at a nominal power density of 2 W/cm^2 and duty cycle of 20%. Tumor growth was then monitored (Fig. 5). In the group treated by microbubble-encapsulated Dox without ultrasound, the tumor growth rate was only slightly slower than in the control group. No statistically significant differences were observed between the control group and that treated by microbubble-encapsulated Dox without ultrasound in a two-tailed unequal variance *t* test ($P = .25$). In contrast, the tumors in the group treated by ultrasound either didn't grow or regressed, and statistically significant differences were observed between the groups treated by microbubble-encapsulated Dox, with and without ultrasound ($P = .001$). Because the drug-loaded microbubbles were injected systemically, the results suggest that without ultrasound, microbubbles tightly retained the drug and that sonication induced a release of the drug from microbubbles, which caused regression of the sonicated tumor.

Microbubbles as Long-Lasting Ultrasound Contrast Agents

Imaging of subcutaneous MDA MB231 human breast cancer tumors grown in mice after intratumoral or intravenous injection of 100 mL of a 0.5% PEG-PLLA/2% PFP microbubble formulation

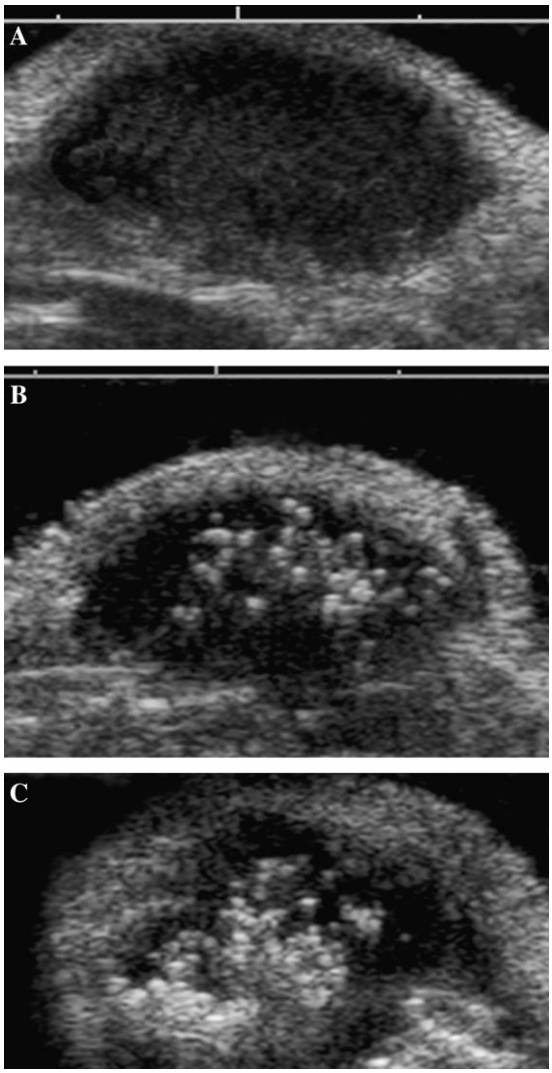

Fig. 6. B-mode ultrasound images of MDA MB231 human breast cancer tumors in nu/nu mice after intratumoral injection of 100 mL 0.5% PEG-PLLA/2% perfluoropentane microbubble formulation. **A**) Ultrasound image taken before the injection. **B** and **C**) Longitudinal and transverse tumor images, respectively taken 4 hours after injection. Images were taken with a 14-MHz linear transducer Acuson Sequoia 512. Strong ultrasound contrast in the tumor was preserved for several days. Note the distribution of echo-producing entities throughout the tumor volume.

(approximately 5×10^8 bubbles/mL) was performed using 14-MHz linear transducer (Acuson Sequoia 512). The resolution limit of this imaging instrument is 0.1 mm; therefore, the nanobubbles or small microbubbles cannot be resolved. Ultrasound images were recorded at 3 minutes, 18 minutes, 4 hours, 28 hours, and 48 hours after injection. Strong echoes were generated in the tumors within one minute after direct intratumoral injection, and they persisted for several days (Fig. 6). The sizes of the echo-producing entities in ultrasound images (100–300 μm) were much larger than the sizes of the nanobubbles in the injected formulation (the injected nanobubbles could not be resolved in ultrasound images). The observation of strong echoes suggested that nanobubbles coalesced in the tumor tissue. This was further confirmed by the results of tumor imaging upon the intravenous injection of the microbubble formulation (Fig. 7). The image presented in Fig. 7, A, was taken

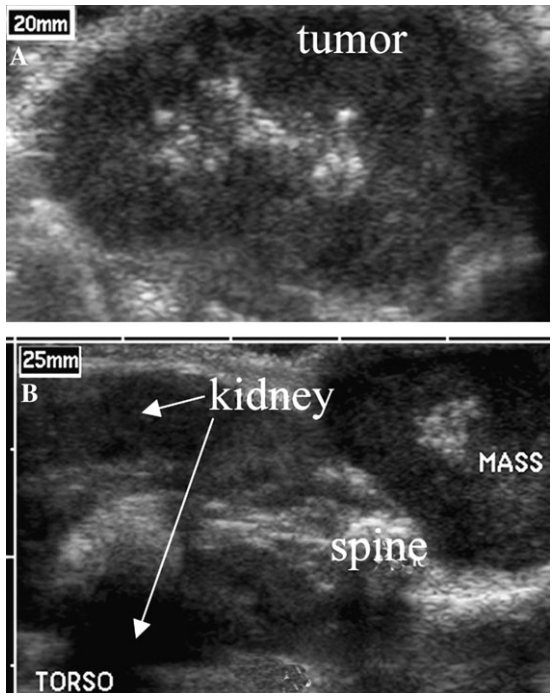

Fig. 7. B-mode ultrasound images of MDA MB231 human breast cancer tumor in a nude mouse after intravenous injection of 100 mL 0.5% PEG-PLLA/2% perfluoropentane microbubble formulation. **A**) Image taken 4.5 hours after injection. **B**) A trans-torso image of the same mouse showing the tumor (designated as "mass"), kidneys, and spine. The images show that echogenic microbubbles accumulated in the tumor but not in the kidneys (or the liver, data not shown).

4 hours after the intravenous injection. It shows a large area of a high echogenicity in the center of the tumor. No accumulation of echogenic microparticles was observed in kidney (Fig. 7, B) or liver, suggesting a high degree of micelle/microbubble tumor targeting.

Although for 3-month grown tumors a substantial ultrasound contrast was generated in the subcutaneous tumors of four mice with the intravenous contrast injection, as illustrated in Fig. 7, A and B, the subcutaneous tumors of two other mice manifested a low number of the echo-producing entities.

In subsequent experiments we took ultrasound images of subcutaneous MDA MB231 breast cancer and A2780 ovarian cancer tumors at 3 and 10 weeks after cell inoculation. No contrast was observed at 3 weeks (tumor size up to 60 mm^3); however, strong contrast was observed 7 weeks later in the large (about 500 mm^3) tumors of the same mice (data not shown). These 10-week tumors had a well developed vasculature that was visible to the naked eye.

Discussion

The micelle/microbubble formulations that we have described fulfilled three important functions: they targeted drugs to tumors, they enhanced the ultrasound-mediated intracellular drug uptake, and they provided a strong and long-lasting tumor contrast in ultrasonography. Each component of the drug delivery system carries out particular functions. Micelles and nanobubbles carry the drug and provide for a selective drug accumulation and retention in the

tumor tissue via the enhanced permeability and retention effect, thus accomplishing passive drug targeting to tumors (4,5). Small nanobubbles encapsulate drugs, extravasate in the tumor tissue, and coalesce into larger, highly echogenic microbubbles, thus providing for a strong tumor contrast in ultrasonography.

In the system we have described, there are a variety of means by which tumor-directed ultrasound could enhance drug uptake. It triggers drug release both from the tumor-accumulated micelles and nano/microbubbles. Because, as shown in our previous work (4,5,7,14,21,22), free drug is internalized by cells more effectively than encapsulated drug, ultrasound-induced drug release from micelles (or bubbles) enhances intracellular drug uptake. Larger microbubbles cavitate under the action of tumor-directed therapeutic ultrasound and by cavitation further enhance intracellular drug uptake by tumor cells. Further enhancement of drug uptake by ultrasound-induced microbubble cavitation is due to its ability to perturb cell membranes (24). Still another important ultrasound-mediated effect is enhancement of the diffusion of nanoparticles and free drug throughout tumor tissue (4,11). Because of the central role of inertial cavitation in enhancing drug uptake, tumor sonication in the presence of microbubbles results in a stronger intracellular drug uptake than in the presence of micelles alone.

The microbubbles we have developed differ in a number of ways from the ultrasound contrast agents currently available, including Optison and Definity: 1) the microbubbles are produced in situ upon injection of a specially designed microemulsion; 2) they have strong walls composed of biodegradable diblock copolymer that stabilizes the microbubbles thus resulting in a long-lasting ultrasonic contrast; 3) the same diblock copolymer that forms the walls of the microbubbles also forms polymeric micelles that effectively encapsulate chemotherapeutic agents and act as drug carriers; and 4) upon drug injection, a localized ultrasonic irradiation of the tumor in the presence of microbubbles provides for effective intracellular drug uptake by the tumor cells.

The therapeutic mechanism of our systems is based on the ultrasound-enhanced localized action of tumor-targeted chemotherapeutic drugs rather than thermal action of ultrasound. This allows the use of ultrasound energies that are at least order of magnitude lower than those used in ablative techniques. A statistically significant enhancement of the intracellular drug uptake was observed at a SATA power density of only 2 W/cm^2 for 3-MHz ultrasound.

It is important to note that selective tumor accumulation of the contrast agent after intravenous injection proceeded without molecular targeting of the microbubbles. The accumulation was based exclusively on the passive targeting of the nanoparticles.

The size of the highly echogenic entities observed in the tumor after the intravenous injections (hundreds of microns) was much larger than the cutoff size of the endothelial gaps in tumor capillaries, which can be up to 750 nm, depending on the tumor type (15,16,32). Therefore, our data strongly suggest that small (200–750 nm) nanobubbles of the initial formulation were extravasated into the tumor and coalesced into larger echogenic microbubbles in the tumor volume. Coalescence of nanobubbles into large microbubbles induced by ultrasound or hyperthermia may be potentially useful for local occlusion of tumor capillaries.

There are limitations of micelle/microbubble systems that are most probably related to the status of the tumor vasculature. An absence or small number of echo-generating entities in the tumors at the early stages of development or in some studied mice with "older" tumors may be related to three possible tumor factors: low vascularization, low cut-off size of the endothelial gaps in tumor blood capillaries that precluded extravasation of the nanobubbles, or structural tumor factors that precluded nanobubble coalescence. Discrimination between these factors requires further research.

In conclusion, multifunctional micelle/microbubble formulations have been developed for combining ultrasonic tumor imaging and ultrasound-enhanced chemotherapeutic treatment. We found that the formulations provide for a long-lasting ultrasound contrast in the tumor tissue, allow tumor visualization via passive targeting of a contrast agent, and enhance the ultrasound-mediated localized drug uptake by the tumor cells.

References

(1) Iyer A, Khaled G, Fang J, Maeda H. Exploiting the enhanced permeability and retention effect for tumor targeting. Drug Discov Today 2006; 11:812–8.

(2) Kabanov A, Alakhov V. Pluronic block copolymers in drug delivery: from micellar nanocontainers to biological response modifiers. Crit Rev Ther Drug Carrier Syst 2002;19:1–72.

(3) Rapoport N, Marin A, Luo Y, Prestwich G, Muniruzzaman M. Intracellular uptake and trafficking of pluronic micelles in drug-sensitive and MDR cells: effect on the intracellular drug localization. J Pharm Sci 2002; 91:157–70.

(4) Rapoport N. Combined cancer therapy by micellar-encapsulated drug and ultrasound. In: Amiji M, editors. Nanotechnology for cancer therapy. Boca Raton (FL): CRC Press; 2006. p. 417–37.

(5) Rapoport N. Tumor targeting by polymeric assemblies and ultrasound activation. In: Arshadi R, Kono K, editors. MML. Vol 8. London (U.K.: Kentus Books; 2006. p. 305–62.

(6) Rapoport N, Herron J, Pitt W, Pitina L. Micellar delivery of doxorubicin and its paramagnetic analog, ruboxyl, to hl-60 cells: effect of micelle structure and ultrasound on the intracellular drug uptake. J Control Release 1999;58:153–62.

(7) Rapoport N, Marin A, Christensen D. Ultrasound-activated micellar drug delivery. Drug Delivery Syst Sci 2002;2:37–46.

(8) Rapoport N, Marin AP, Timoshin AA. Effect of a polymeric surfactant on electron transport in hl-60 cells. Arch Biochem Biophys 2000; 384:100–8.

(9) Rapoport N, Pitina L. Intracellular distribution and intracellular dynamics of a spin-labeled analogue of doxorubicin by fluorescence and EPR spectroscopy. J Pharm Sci 1998;87:321–5.

(10) Rapoport N, Pitt WG, Sun H, Nelson JL. Drug delivery in polymeric micelles: from in vitro to in vivo. J Control Release 2003;91:85–95.

(11) Gao Z, Fain H, Rapoport N. Controlled and targeted tumor chemotherapy by micellar-encapsulated drug and ultrasound. J Control Release 2005;102:203–21.

(12) Gao Z, Fain HD, Rapoport N. Ultrasound-enhanced tumor targeting of polymeric micellar drug carriers. Mol Pharm 2004;1:317–30.

(13) Allen C, Maysinger D, Eisenberg A. Nano-engineering block copolymer aggregates for drug delivery. Colloids Surf B Biointerfaces 1999;16:3–27.

(14) Howard B, Gao Z, Rapoport N. Ultrasound-enhanced chemotherapy of drug resistant breast cancer tumors by micellar-encapsulated paclitaxel. Am J Drug Deliv 2006;4:97–104.

(15) Hobbs S, Monskey W, Yuan F, Roberts G, Griffith L, Torchilin V, et al. Regulation of transport pathways in tumor vessels: role of tumor type and microenvironment. Proc Natl Acad Sci U S A 1998;95:4607–12.

(16) Campbell R. Tumor physiology and delivery of nanopharmaceuticals. Anticancer Agents Med Chem 2006;6:503–12.

(17) Bamber JC. Attenuation and absorption. In: Hill CR, Bamber JC, ter Haar GR. Physical principles of medical ultrasonics. Chichester (U.K.): John Wiley & Sons; 2004. p. 118–9.
(18) Husseini GA, Myrup GD, Pitt WG, Christensen DA, Rapoport NY. Factors affecting acoustically triggered release of drugs from polymeric micelles. J Control Release 2000;69:43–52.
(19) Husseini G, Rapoport N, Christensen D, Pruitt J, Pitt W. Kinetics of ultrasonic release of doxorubicin from pluronic p-105 micelles. Colloids Surf B Biointerfaces 2002;24:253–64.
(20) Marin A, Muniruzzaman M, Rapoport N. Acoustic activation of drug delivery from polymeric micelles: effect of pulsed ultrasound. J Control Release 2001;71:239–49.
(21) Marin A, Muniruzzaman M, Rapoport N. Mechanism of the ultrasonic activation of micellar drug delivery. J Control Release 2001;75:69–81.
(22) Marin A, Sun H, Husseini GA, Pitt WG, Christensen DA, Rapoport NY. Drug delivery in pluronic micelles: effect of high-frequency ultrasound on drug release from micelles and intracellular uptake. J Control Release 2002;84:39–47.
(23) Rapoport N. Factors affecting ultrasound interactions with polymeric micelles and viable cells. In: Swenson S, editor. Carrier-based drug delivery. Vol 879. Washington (DC): ACS Symposium Series; 2004. p. 161–73.
(24) Kamaev P, Rapoport N. Effect of anticancer drug on cell sensitivity to ultrasound in vitro and in vivo. Am J Phys 2006;829:543–5.
(25) Rapoport N, Christensen D, Fein H, Barrows L, Gao Z. Ultrasound-triggered drug targeting to tumors in vitro and in vivo. Ultrasonics 2004;42:943–50.
(26) Rapoport N. Controlled drug delivery to drug-sensitive and multidrug resistant cells: effects of pluronic micelles and ultrasound. In: Dinh SM, Liu P, editors. Advances in controlled drug delivery. Vol 846. Washington (DC): ACS Symposium Series; 2003. p. 85–101.
(27) Rapoport N. Stabilization and acoustic activation of pluronic micelles for tumor-targeted drug delivery. Colloids Surf B Biointerfaces 1999;3:93–111.
(28) Lo A, Kripfgans O, Carson P, Fowlkes J. Spatial control of gas bubbles and their effects on acoustic fields. Ultrasound Med Biol 2006;32:95–106.
(29) Kripfgans O, Fabiilli M, Carson P, Fowlkes J. On the acoustic vaporization of micrometer-sized droplets. J Acoust Soc Am 2004;116:272–81.
(30) Kripfgans O, Fowlkes J, Miller D, Eldevik O, Carson P. Acoustic droplet vaporization for therapeutic and diagnostic applications. Ultrasound Med Biol 2000;26:1177–89.
(31) Husseini GA, Diaz de la Rosa MA, Richardson ES, Christensen DA, Pitt WG. The role of cavitation in acoustically activated drug delivery. J Control Release 2005;107:253–61.

Funding

National Institutes of Health (R01 EB1033 to N. Rapoport).

Notes

The authors are grateful to Aniko Szabo (Director, Biostatistic Shared Resource, Huntsman Cancer Institute) for the statistical analysis of the data. We thank a graduate student Praveena Mohan for participation in fluorescence imaging experiments.

The study sponsors had no role in the design of the study; the collection, analysis, and interpretation of the data; the writing of the manuscript; or the decision to submit the manuscript for publication.

Manuscript received September 28, 2006; revised April 30, 2007; accepted June 7, 2007.